Angewandte International Edition Chemie

Service

Author Profile

"My mottos are 'be naïve' and 'be creative'. My favorite way to spend a holiday is fishing in a mountain stream. …"
This and more about Noritaka Mizuno can be found on page 10442.

News


C. P. R. Hackenberger


A. J. von Wangelin


P. S. Baran


N. Garg


A. Doyle

Obituaries

Ivano Bertini, one of the pioneers of bioinorganic chemistry, recently passed away at the age of 71. His work on determining the solution structures of the metalloproteins with paramagnetic centers was one of his many achievements.

Books

Highlights

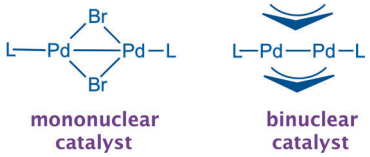

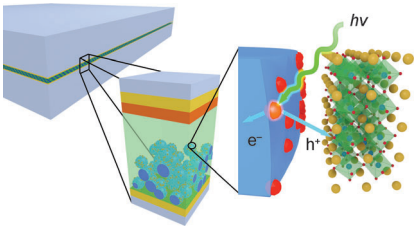

Correspondence

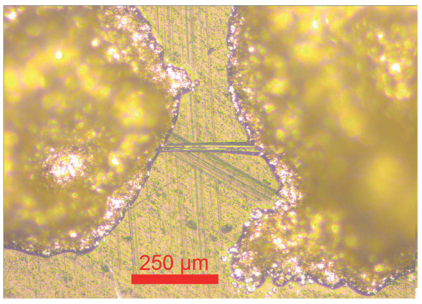

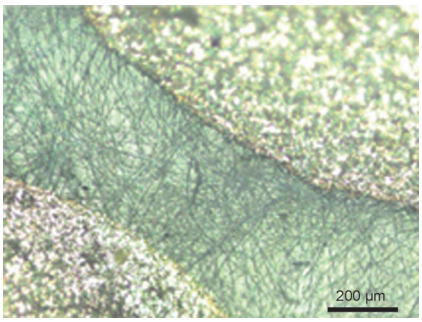

For the USA and Canada:
ANGEWANDTE CHEMIE International Edition (ISSN 1433-7851) is published weekly by Wiley-VCH, PO Box 191161, 69451 Weinheim, Germany. Air freight and mailing in the USA by Publications Expediting Inc., 200 Meacham Ave., Elmont, NY 11003. Periodicals postage paid at Jamaica, NY 11431. US POSTMASTER: send address changes to *Angewandte Chemie*, Journal Customer Services, John Wiley & Sons Inc., 350 Main St., Malden, MA 02148-5020. Annual subscription price for institutions: US$ 11.738/10.206 (valid for print and electronic / print or electronic delivery); for individuals who are personal members of a national chemical society prices are available on request. Postage and handling charges included. All prices are subject to local VAT/sales tax.

Minireviews

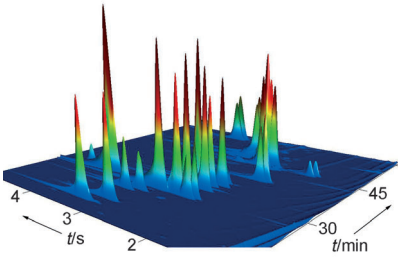

Dimension jump: The ability to obtain multidimensional chromatograms by passing analytes over two different stationary phases connected by a modulator led to the invention of comprehensive gas chromatography. The increased resolution offered by GC×GC techniques (see picture) compared to that of traditional GC is useful for multiple applications, including the resolution of enantiomers.

Reviews

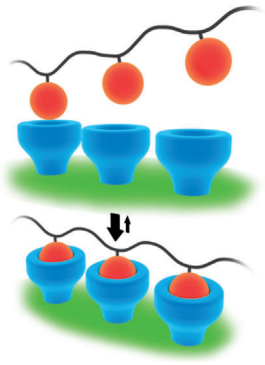

Unified strength: Multivalent structures function in a number of biological systems to generate a strong but reversible interaction between two objects. The chemical realization of this natural principle with organized multiple interactions enables, for example, the development of multivalent drugs for an effective inhibition of viral cell attachment.

Communications

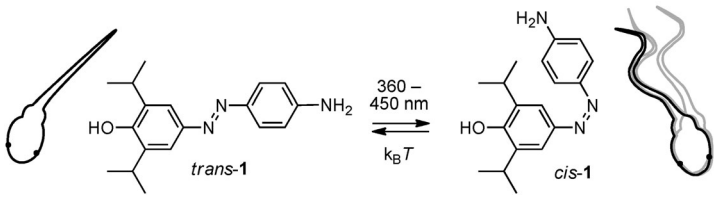

Shine and rise! $GABA_A$ receptors are ligand-gated chloride ion channels that respond to γ-aminobutyric acid (GABA), which is the major inhibitory neurotransmitter of the mammalian central nervous system. Azobenzene derivatives of propofol, such as compound **1** (see scheme), increase GABA-induced currents in the dark form and lose this property upon light exposure and thus function as photochromic potentiators. Compound **1** can be employed as a light-dependent general anesthetic in translucent tadpoles.

The German Chemical Society (GDCh) invites you to:

Angewandte Anniversary Symposium

125 JAHRE Eine Zeitschrift der Gesellschaft Deutscher Chemiker

GDCh

Tuesday, March 12, 2013

Henry Ford Building / FU Berlin

Speakers

Carolyn R. Bertozzi

François Diederich

Alois Fürstner

Roald Hoffmann (Nobel Prize 1981)

Susumu Kitagawa

Jean-Marie Lehn (Nobel Prize 1987)

E.W. "Bert" Meijer

Frank Schirrmacher (Publisher, *FAZ*)

Robert Schlögl

George M. Whitesides

Ahmed Zewail (Nobel Prize 1999)

More information:

Freie Universität Berlin

angewandte.org/symposium

WILEY-VCH

GDCh Gesellschaft Deutscher Chemiker

PSJ_12_42497_5_gu

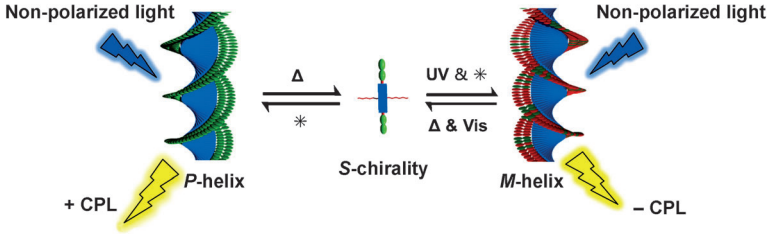

Spiraling into control: A photoresponsive supramolecular assembly demonstrates that light, along with heating (Δ) and cooling (✳), can cause chiral communication between molecules. This effect leads to bias in the helicity of the complex, causing a reversible switching of macroscopic handedness, as shown by a reversal of sign of the circularly polarized luminescence (CPL) that is emitted.

Photoswitchable Helicity

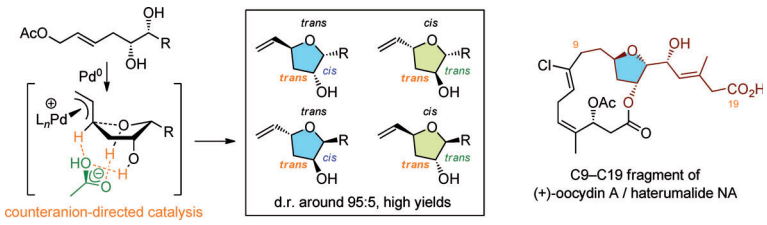

Hydrogen bonds can play a prominent role in organometallic catalysis, as shown for the title reaction, in which a counteranion directs the cyclization through the formation of hydrogen bonds that likely involve a proton of the π-allyl/palladium species itself. The reaction allows access to four out of the eight stereoisomers of 2,5-disubstitued 3-hydroxy-tetrahydrofurans and thus fragments of complex natural products.

Stereoselective Catalysis

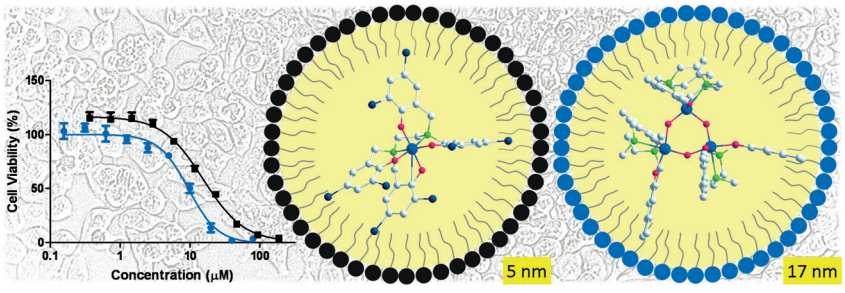

A nanoformulated trinuclear hydrolysis product of a bis(alkoxo) salan–Ti^{IV} complex shows high antitumor activity (see picture), which identifies it as an active species in cells. Additional highly stable mononuclear derivatives also show high activity, when formulated into nanoparticles, thus evincing that biologically friendly Ti^{IV} can provide high cytotoxicity with controlled biological function.

Drug Discovery

Single-Molecule Imaging

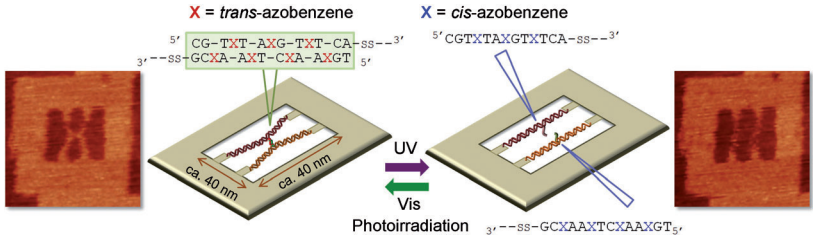

A framed photo of DNA: A pair of photoresponsive oligonucleotides containing azobenzene moieties was introduced into double-stranded DNA within the cavity of a DNA nanostructure (see scheme). The two dsDNAs, in contact at the center, were dissociated using UV irradiation and hybridized with visible light; this was directly observed using high-speed atomic force microscopy.

Quantum Dot Biolabeling

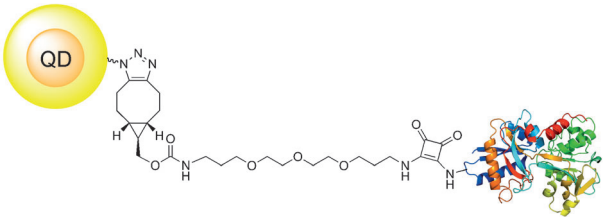

Twinkle twinkle quantum dot: Conjugation of biomolecules to azide-modified quantum dots (QDs) through a bifunctional linker, using strain-promoted azide–alkyne cycloaddition with the QD and a squaramide linkage to the biomolecule (see scheme). Transferrin-conjugated QDs were internalized by transferrin-receptor expressing HeLa cells.

CO_2 Fixation

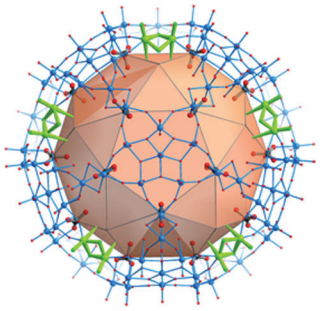

30 receptors in waiting position: In the porous $(pentagon)_{12}(linker)_{30}$-type molybdenum oxide capsule (see picture), the 30 positively charged linkers (five unsaturated shown for illustration in green, the others contain CO_3^{2-} ligands) can act as receptors for neutral and negatively charged ligands. Bubbling CO_2 into the solution containing the acetate-type capsules leads to the upload of CO_2 based on 30 coordinated CO_3^{2-} ligands.

Antibiotic Resistance

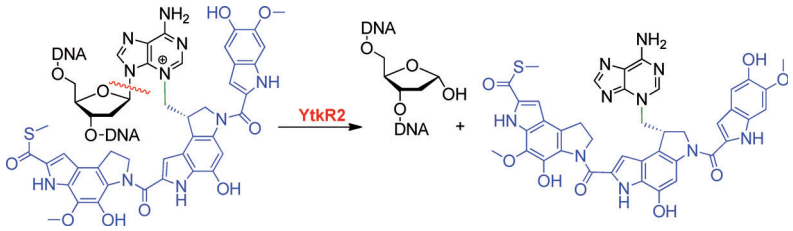

Resistance is (not) futile: The yatakemycin biosynthetic gene cluster involves the *ytkR2* gene, which encodes a protein with homology to a recently discovered bacterial DNA glycosylase. Genetic validation in vivo, biochemical assays, and in vitro mutagenesis studies revealed that YtkR2 confers resistance for the bacteria by specifically recognizing and cleaving the YTM-modified base (see scheme).

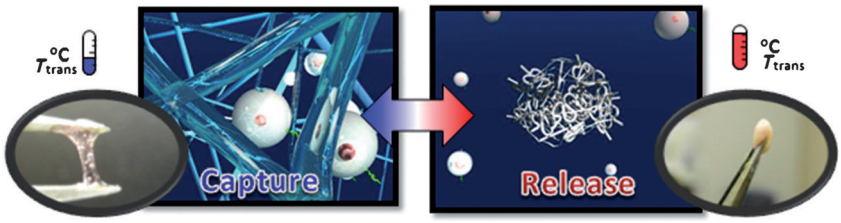

Caught in a web: Photo-cross-linkable temperature-responsive polymer-based nanofiber webs have been synthesized that have the ability to capture, encapsulate, and release cells by dynamically transforming the fibrous structure into hydrogel-like structures by wrapping, swelling, and deswelling processes in response to external temperature changes (see picture).

Smart Materials

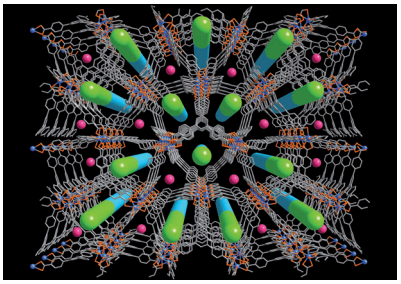

Frequency doubling: A strategy for incorporating dipolar organic chromophores into the one-dimensional channels of an anionic metal–organic framework (MOF) has been developed to generate highly active nonlinear optical materials (see picture). The resulting MOF material shows a second-harmonic generation intensity of 18.3 versus α quartz.

Metal–Organic Frameworks

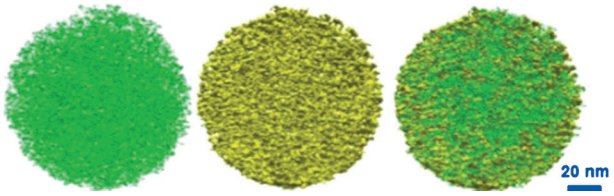

From droplets to "spheres": A platform technology enables the rapid and continuous synthesis of mesoporous metal and metal alloy particles (see picture). The confined growth of nanocrystals in aerosol droplets leads to the formation of these particles with defined composition.

Nanocrystal Networks

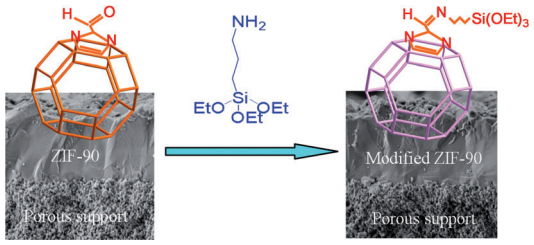

A clear separation: A post-synthetic functionalization method is reported to obtain a highly permselective zeolitic imidazolate framework (ZIF-90) membrane. The intercrystalline defects of the ZIF-90 membrane are minimized to enhance the separation selectivity while a high permeance is maintained.

Metal–Organic Frameworks

Drug-Carrying Nanoparticles

Learning to let go with age: Intracellular controlled release of molecules within senescent cells was achieved using mesoporous silica nanoparticles (MSNs) capped with a galacto-oligosaccharide (GOS) to contain the cargo molecules (magenta spheres; see scheme). The GOS is a substrate of the senescent biomarker, senescence-associated β-galactosidase (SA-β-gal), and releases the cargo upon entry into SA-β-gal expressing cells.

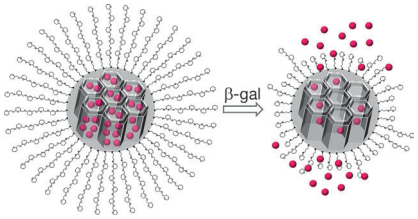

Materials Science

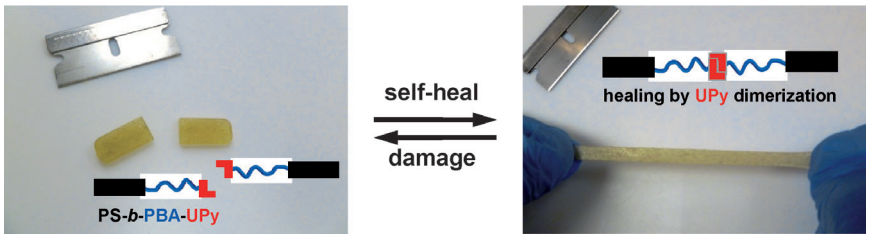

Polymer, heal thyself! Supramolecular ABA triblock copolymers formed by dimerization of 2-ureido-4-pyrimidinone (UPy) end-functionalized polystyrene-*b*-poly(*n*-butyl acrylate) (PS-*b*-PBA) AB diblock copolymers have been synthesized, resulting in a self-healing material that combines the advantageous mechanical properties of thermoplastic elastomers and the dynamic self-healing features of supramolecular materials.

Gel Nanocubes

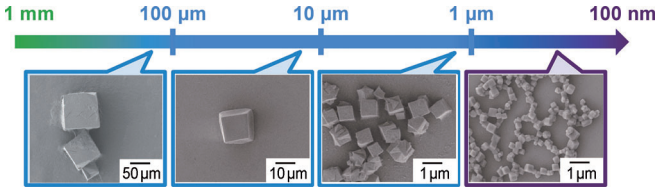

Sweet cube o' mine: Bottom-up control of gel particles has been regarded as a great challenge. By employing internal cross-linking of cyclodextrin metal–organic frameworks, cubic sugar gels were formed with sharp edges that reflect the shape of the crystals. This enabled the fabrication of shape- and size-controlled polymer gels from porous crystals (see picture).

Bionanotechnology

Lightening organelles: A femtosecond laser can excite multiphoton-induced luminescence of graphene oxide nanoparticles. The flow, distributions, and clearance of intravenously injected GO-PEG nanoparticles in the blood vessel of mice could be observed clearly by two-photon imaging. The 3D distribution of microinjected GO-PEG nanoparticles in a mice brain could also be reconstructed with two-photon microscopy.

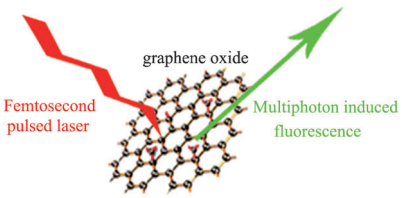

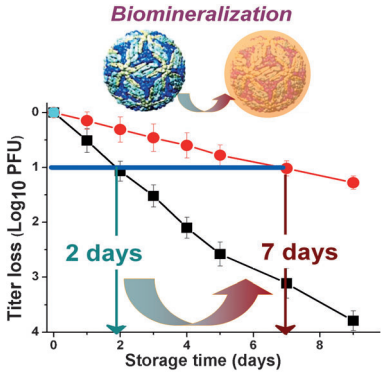

We're not gonna bake it: In situ biomineralization creates an egg-like shell on vaccine particles to improve their thermostability. Different from the bare vaccine (squares), the biomineralized vaccine (red circles) can be stored at ambient temperature without refrigeration for up to a week and retain biological activity both in vitro (see graph), as well as in a mouse model.

Vaccine Stabilization

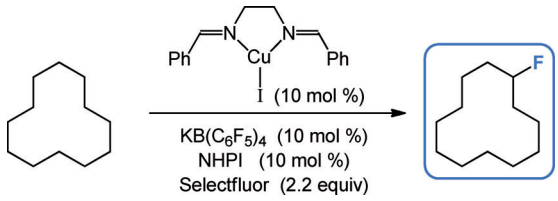

A group effort: Reported is the title reaction using a polycomponent catalytic system involving commercially available Selectfluor, a putative radical precursor *N*-hydroxyphthalimide, an anionic phase-transfer catalyst ($KB(C_6F_5)_4$), and a copper(I) bis(imine). The catalyst system formed leads to monofluorinated compounds selectively (see example) without the necessity for an excess of the alkane substrate.

Synthetic Methods

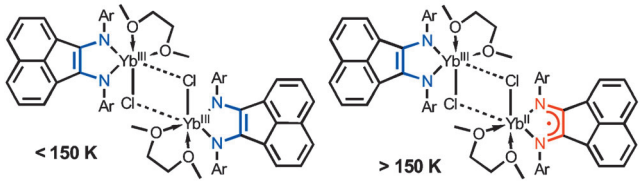

Redox isomerism is observed for a lanthanide complex for the first time. Upon lowering the temperature, an electron of $[\{(dpp\text{-}bian)Yb(\mu\text{-}Cl)(dme)\}_2]$ (**1**) is transferred from the metal to the ligand (see picture), giving rise to marked shortening of Yb–N bonds and a hysteretic jump in the magnetic moment. The crystal packing is of a crucial importance, as two other crystal modifications of **1** do not undergo this effect.

Rare Earths

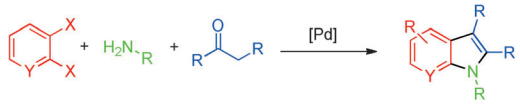

Highly substituted indoles were synthesized by a palladium-catalyzed reaction involving three independent components in a one-pot reaction. Two distinct palladium-catalyzed coupling reactions occur with a single catalytic system: a Buchwald-Hartwig reaction and an arene-alkene coupling. Quantum chemical computations provide insight into the mechanism of the latter coupling step.

Indole Synthesis

Asymmetric Synthesis

Regio- and Enantioselective Cobalt-Catalyzed Reductive [3+2] Cycloaddition Reaction of Alkynes with Cyclic Enones: A Route to Bicyclic Tertiary Alcohols

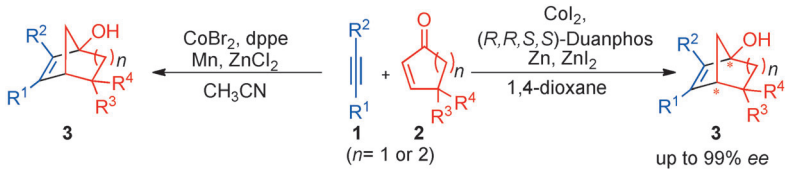

Round and round: An unusual cobalt-catalyzed regio- and enantioselective reductive [3+2] cycloaddition of cyclic enones with alkynes affording bicyclic tertiary alcohols is described. A possible mechanism involving the formation of a cobaltacyclopentene intermediate is proposed.

Natural Product Synthesis

Enantioselective Formal Total Syntheses of Didehydrostemofoline and Isodidehydrostemofoline through a Catalytic Dipolar Cycloaddition Cascade

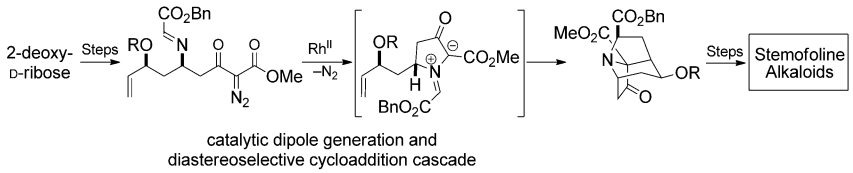

Sweet to the core: Enantioselective formal total syntheses of the title compounds were accomplished in 24 steps from 2-deoxy-D-ribose. The synthesis features a novel cascade of reactions culminating in an intramolecular dipolar cycloaddition to form the tricyclic core of the stemofoline alkaloids from an acyclic diazo imine intermediate.

Bioorthogonal Chemistry

Genetically Encoded Cyclopropene Directs Rapid, Photoclick-Chemistry-Mediated Protein Labeling in Mammalian Cells

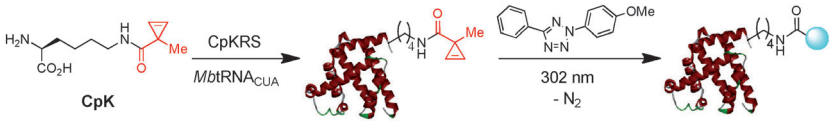

We just click: Genetic incorporation of a cyclopropene amino acid CpK (see scheme) site-specifically into proteins in *E. coli* and mammalian cells was achieved using an orthogonal aminoacyl-tRNA synthetase/$tRNA_{CUA}$ pair (CpKRS/$MbtRNA_{CUA}$). Cyclopropene exhibited fast reaction kinetics in the photoclick reaction and allowed rapid (ca. 2 min) labeling of proteins.

Carbenoids

A Nonmetal Approach to α-Heterofunctionalized Carbonyl Derivatives by Formal Reductive X–H Insertion

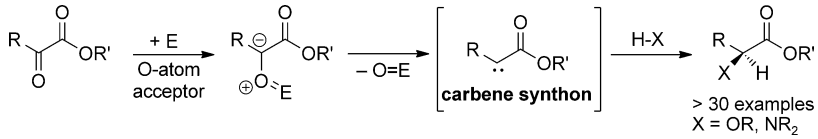

Keeping it organic: A direct synthesis of α-alkoxy and α-amino ester derivatives by direct reductive coupling of widely available, stable α-keto esters and protic pronucleophiles is described (see scheme; X = OR, NR_2). The method serves as a convenient nonmetal alternative to X–H insertion by diazo decomposition.

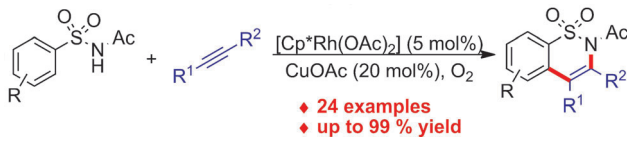

Director's cut: The pharmaceutically relevant sulfonamide group is shown to be a competent directing group for [Cp*Rh(OAc)$_2$]-catalyzed C–H functionalizations. Reactions of the cyclometalated intermediate with internal alkynes provide access to a wide range of sultam derivatives. The reaction is high yielding and works best under aerobic conditions with catalytic amounts of CuOAc as an oxidation mediator. Cp* = C_5Me_5.

Homogenous Catalysis

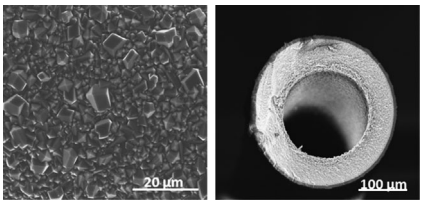

Headed for a membrane: Continuous, polycrystalline ZIF-90 membranes (picture, left) can be grown at 65 °C from methanolic precursor solutions on nanocrystal-seeded surfaces of poly(amide–imide) macroporous hollow fibers (right). The ZIF-90 membranes exhibit good separation properties for linear over cyclic hydrocarbons, as well as gas permeation selectivities higher than Knudsen values.

Membrane Fabrication

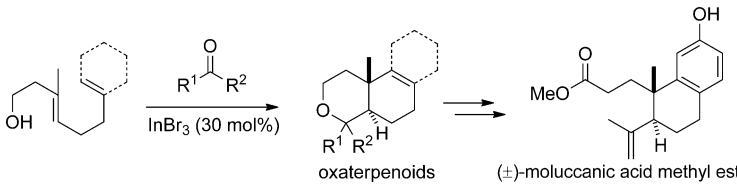

Cascades: An $InBr_3$-catalyzed intermolecular polyene cyclization initiated by a Prins reaction provides a concise approach to 3-oxaterpenoid derivatives. The reaction is compatible with various aldehydes, ketones, and polyolefin–alcohol substrates. In addition, the total synthesis of (±)-moluccanic acid methyl ester was achieved in seven steps by using such a Prins–polyene cyclization as the key step.

Synthetic Methods

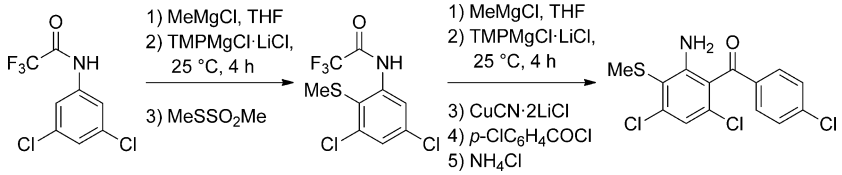

A practical *ortho*,*meta*, (or even *ortho*,*ortho'*) magnesiation of trifluoroacetamides of anilines, aminopyridines, and aminopyrazines at room temperature was performed with TMPMgCl·LiCl or $TMP_2Mg{\cdot}2\,LiCl$. These magnesiations are compatible with several carbonyl functionalities and allow access to polysubstituted anilides in satisfactory yields.

Synthetic Methods

Gold Fluorides

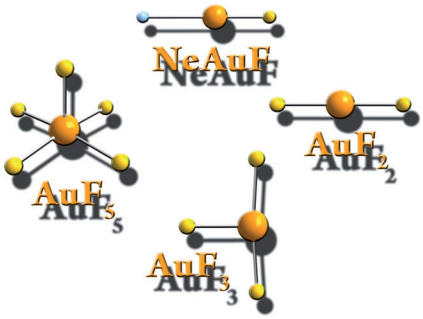

Noble with a difference: Matrix-isolation experiments and quantum-chemical calculations have led to the characterization of two new compounds, namely first open-shell binary gold fluoride, AuF_2, and a NeAuF complex. Moreover, ArAuF, AuF_3, Au_2F_6, and monomeric AuF_5 have been produced and identified under cryogenic conditions in neon and argon matrices.

Dual Activation

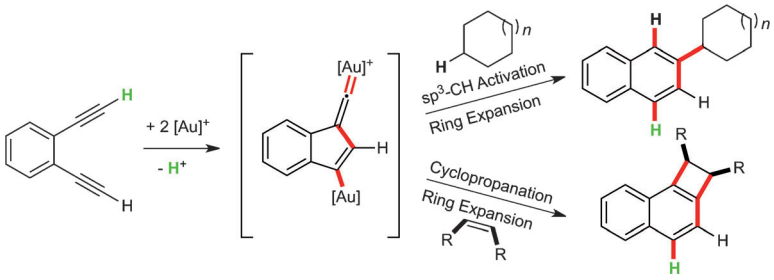

Highly reactive gold vinylidene species are used for intermolecular C(sp³)–H insertions into unactivated alkanes (see scheme). In addition, they can be regarded as synthons for alkylidene carbenes. Initiated by cyclopropanation of the vinylidene species/alkylidene carbenoide, cyclobutene derivatives are formed in a diastereoselective fashion by a ring-enlargement cascade in only one step.

Biosynthesis

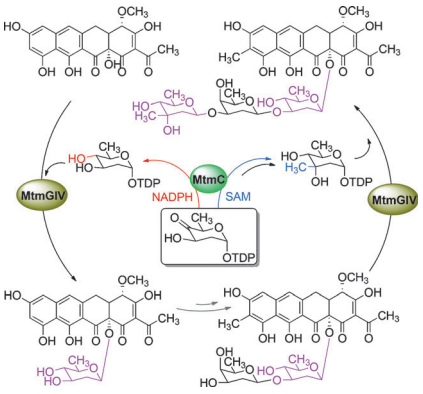

Two bifunctional enzymes cooperate in the assembly and the positioning of two sugars, D-olivose and D-mycarose, of the anticancer antibiotic mithramycin. MtmC finishes the biosynthesis of both sugar building blocks depending on which MtmGIV activity is supported. MtmGIV transfers these two sugars onto two structurally distinct acceptor substrates. The dual function of these enzymes explains two essential but previously unidentified activities.

Gold(III) Hydrides

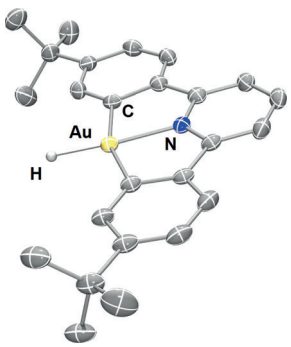

Going for gold: The first thermally stable gold(III) hydride [(C^N^C)*AuH] is presented. It undergoes regioselective insertions with allenes to give gold(III) vinyl complexes, and reductive condensation with [(C^N^C)*AuOH] to the air-stable Au^{II} product, $[(C^N^C)^*{}_2Au_2]$, with a short nonbridged gold–gold bond.

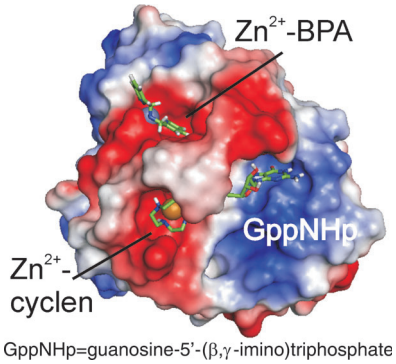

GppNHp=guanosine-5'-(β,γ-imino)triphosphate

Allosteric interactions: Metal(II) cyclens inhibit Ras–effector interactions by stabilizing a weak effector-binding state of Ras, state 1(T), and binding directly in the active site. The novel state (1T) inhibitor Zn^{2+}–BPA (BPA = bis(2-picolyl)amine) binds outside the nucleotide binding pocket but nevertheless allosterically stabilizes state 1(T) and thus inhibits the Ras–Raf interaction.

Inhibitors

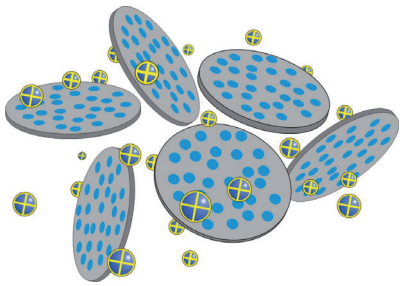

The neutral organic dye indigo forms an inorganic–organic hybrid material with nanoclays (see picture; blue circles on disks symbolizing indigo, spheres indicating liberated cations) and can thus be transferred into aqueous solution. Solids recovered from these solutions resemble the ancient Maya Blue pigment. The method can also be applied to other hydrophobic species and may open the gate for novel solution chemistry, including photonic and catalytic applications.

Water Solubilized Indigo

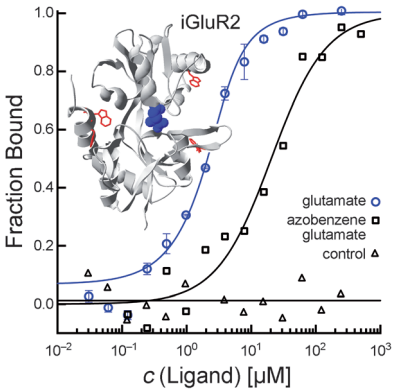

Look, no label! Microscale thermophoresis makes use of the intrinsic fluorescence of proteins to quantify the binding affinities of ligands and discriminate between binding sites. This method is suitable for studying binding interactions of very small amounts of protein in solution. The binding of ligands to iGluR membrane receptors, small-molecule inhibitorss to kinase p38, aptamers to thrombin, and Ca^{2+} ions to synaptotagmin was quantified.

Protein–Ligand Interactions

Shake it up baby! Simply shaking a polymer-supported reagent and the racemic amine at room temperature kinetically resolves a broad range of N-heterocycles with good selectivity. The polymer-supported reagents are robust, easy to regenerate, and can be reused dozens of times. Cleavable acyl groups can be used to give access to both amine enantiomers in a single resolution.

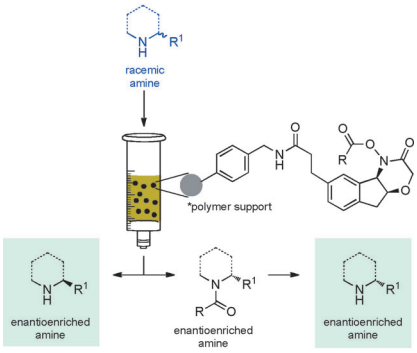

Enantioenriched Amines

Combinatorial Biosynthesis

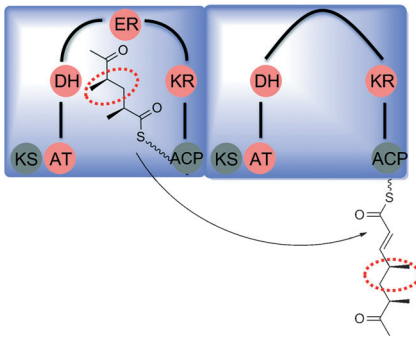

Not in the public domain: Site-directed mutagenesis of megasynthases was the key to the generation of a library of polyketides in bacteria. Redox derivatizations are used to change the bioactivity profile of the compounds.

Supporting information is available on www.angewandte.org (see article for access details).

A video clip is available as Supporting Information on www.angewandte.org (see article for access details).

This article is available online free of charge (Open Access).

This article is accompanied by a cover picture (front or back cover, and inside or outside).

Angewandte Corrigendum

Formal Asymmetric Synthesis of Echinopine A and B

Angew. Chem. Int. Ed. **2011**, *50*

DOI: 10.1002/anie.201008000

The authors of this communication wish to cite additional publications as reference [4b–f]. The complete reference [4] is shown below.

[4] a) V. Michelet, P. Y. Toullec, J.-P. Genet, *Angew. Chem.* **2008**, *120*, 4338 – 4386; *Angew. Chem. Int. Ed.* **2008**, *47*, 4268 – 4315. For pioneering studies in palladium-mediated enyne cycloisomerizations and subsequent cycloadditions, see: b) B. M. Trost, M. Lautens, *J. Am. Chem. Soc.* **1985**, *107*, 1781 – 1783; c) B. M. Trost, J. Y. L. Chung, *J. Am. Chem. Soc.* **1985**, *107*, 4586 – 4588; d) B. M. Trost, D. T. MacPherson, *J. Am. Chem. Soc.* **1987**, *109*, 3483 – 3484; e) B. M. Trost, G. J. Tanoury, M. Lautens, C. Chan, D. T. MacPherson, *J. Am. Chem. Soc.* **1989**, *116*, 4255 – 4267; f) B. M. Trost, P. A. Hipskind, J. Y. L. Chung, C. Chan, *Angew. Chem.* **1989**, *101*, 1559 – 1561; *Angew. Chem. Int. Ed. Engl.* **1989**, *28*, 1502 – 1504.

Polarization Rotation in the Monoclinic Perovskite $BiCo_{1-x}Fe_xO_3$

Angew. Chem. Int. Ed. **2012**, *51*

DOI: 10.1002/anie.201202644

The wrong tilting angles of polarization vector were shown in this Communication. The polarization tilts in the same direction to the monoclinic distortion, and the correct tilting angles are −2° for $x = 0.63$, 12° for $x = 0.70$, and 15° for $x = 0.72$ from $[001]_m$ direction, corresponding to −1° for $x = 0.63$, 13° for $x = 0.70$, and 17° for $x = 0.72$ from $[001]_c$ direction. Figure 5 is accordingly corrected. The authors apologize for this mistake and any inconvenience it may have caused.

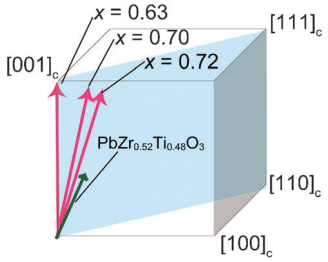

Figure 5. The polarization vectors of the monoclinic *Cm* phase of $BiCo_{1-x}Fe_xO_3$ ($x = 0.63$, 0.70, and 0.72) at 300 K and $PbZr_{0.52}Ti_{0.48}O_3$ at 20 K.[2b] The indices $[001]_c$, $[100]_c$, $[110]_c$, and $[111]_c$ are based on the pseudo cubic unit cell.

Angewandte Addition

The authors of this communication wish to add the following sentence to their acknowledgement:
"V.G. acknowledges the support of DOE grant DE-SC0002040."

C–H Activation in S-Alkenyl Sulfoximines: An Endo 1,5-Hydrogen Migration

X. Gao, V. Gaddam, E. Altenhofer, R. R. Tata, Z. Cai, N. Yongpruksa, A. K. Garimallaprabhakaran, M. Harmata* ——— **7016–7019**

Angew. Chem. Int. Ed. **2012**, *51*

DOI: 10.1002/anie.201203258